

Reduced basal activity and increased functional homogeneity in sensorimotor and striatum of a Parkinson's disease rat model: a functional MRI study

Galit Pelled,¹ Hagai Bergman,² Tamir Ben-Hur³ and Gadi Goelman¹

¹MRI/MRS lab, the Human Biology Research Center, Department of Medical Biophysics, and ³Department of Neurology, the Agnes Ginges Center for Human Neurogenetics, Hadassah Hebrew University Medical Center, Jerusalem, Israel

²Department of Physiology, Hadassah Medical School and the Eric Roland Center for Neurodegenerative Diseases, The Hebrew University, Jerusalem, Israel

Keywords: 6-OHDA, fMRI, Parkinson's disease, physiological noise, rat

Abstract

Functional neuro-imaging studies of Parkinson's disease (PD) patients and animal models show inconsistent cortical responses to sensory stimulation: some present increased sensorimotor cortex activation contradicting classical basal ganglia–cortex circuitry models, whereas others show decreased activation. As functional neuro-imaging activation is defined as the signal difference between stimulation ON and stimulation OFF, reduced 'activation' can point to either increased neuronal activity during stimulation ON or to decreased basal neuronal activity during stimulation OFF. A unique non-invasive method that uses the temporal and the spatial variances of functional magnetic resonance imaging signal is employed here to compare basal neuronal activity levels and 'functional homogeneity' between groups. Based on the assumption that the temporal variance reflects average neuronal activity, the variance of activity within a predefined region is defined as the region's 'functional homogeneity', which is assumed to estimate neuronal synchronization. Comparison of temporal and spatial variances of the sensorimotor cortex and the striatum in the 6-hydroxydopamine (6-OHDA) PD rat model and a control rat group show bilaterally decreased temporal and spatial variances in the 6-OHDA rat group, suggesting bilateral reduction of basal neuronal activity levels together with an increase in local neuronal synchronization in line with classical basal ganglia–cortex circuit models.

Introduction

Functional imaging studies of Parkinson's disease (PD) patients show inconsistent sensorimotor cortex activation as a result of sensory stimulation. Using positron emission tomography (PET) (Jenkins *et al.*, 1992; Playford *et al.*, 1992; Jahanshahi *et al.*, 1995), reduced activity in motor-related areas in human PD subjects has been observed, whereas other studies using functional magnetic resonance imaging (fMRI) (Sabatini *et al.*, 2000), PET (Brooks, 1999; Catalan *et al.*, 1999) and single photon emission tomography (SPECT) (Rascol *et al.*, 1997) have reported increased activation. As the latter results contradict classical models of the basal ganglia (BG) cortex circuitry (Albin *et al.*, 1989; DeLong, 1990), we have previously used well-controlled electric forepaw sensory stimulation to minimize stimulation variability in a study of the unilateral 6-hydroxydopamine (6-OHDA) rat model of PD (Pelled *et al.*, 2002). This revealed a bilateral increase in sensorimotor cortex activation, and indicating a critical difference between neuro-imaging and the predictions of classical models. However, because functional imaging gives a relative measure equal to the signal difference between stimulation ON and stimulation OFF, reduced activation during stimulation OFF

(hereafter referred to as the basal activity level) as well as an increase in neuronal activity during stimulation ON can account for the observation of an 'activation' increase. In order to discriminate between these two scenarios, one of which supports the classical view whereas the other challenges it, a method to measure basal activity level is required. Here we use and extend our recently introduced non-invasive method that estimates basal activity level by using physiological MRI noise (Pelled & Goelman, 2004) and compare basal activity levels in control and PD rat groups.

Extraction of physiological information from low-frequency MRI temporal fluctuations has been used to measure functional connectivity between different cerebral volumes in normal and pathological conditions (Biswal *et al.*, 1995, 1997; Buchel & Friston, 1997, 1998). The low frequencies of these temporal fluctuations can be used to identify regions of synchronized activity, thus indicating areas that are functionally connected. It has also been shown that the signal temporal variance is a function of different MRI parameters such as the echo time (TE) and repetition time (TR) (Kruger & Glover, 2001) similar to the blood oxygenation level-dependent (BOLD) contrast, suggesting that fMRI temporal variance could be used as a means of comparing basal activity levels between groups. Recently, we have tested this approach and demonstrated its sensitivity by showing significant differences between rat visual cortical laminas. We have shown that the differences between temporal variances of the rat

Correspondence: Dr G. Goelman, as above.
E-mail: gadig@hadassah.org.il

Received 2 December 2004, revised 2 February 2005, accepted 6 February 2005

cortical lamina during spontaneous activity (stimulation OFF) is highly congruent with published electrophysiological recordings (Pelled & Goelman, 2004).

We have (1) used the temporal variance approach to show a reduction in basal activity level in the sensorimotor cortex and the striatum of PD rats compared with control rats, and (2) extended the method to obtain an estimation of local neuronal synchronization, here termed 'functional homogeneity'. Comparing the functional homogeneity in the sensorimotor and striatum between PD and control rat groups can indicate a change in local neuronal synchronization in Parkinsonism, which is in line with recent electrophysiological studies (Goldberg *et al.*, 2002).

Material and methods

Animal procedures

The unilateral 6-OHDA rat model of PD was used. Twenty-five male Sprague–Dawley rats, weighing 250–300 g, were used in the study. Fifteen rats were anaesthetized with ketamine (90 mg/kg *i.p.*, Park-Davis, UK) and xylazine (5 mg/kg *i.p.*, Vitamed, Israel) and stereotaxically injected into either the right (eight rats) or the left (seven rats) substantia nigra pars compacta (SNc) with 4 μ L of 10 mM 6-OHDA hydrobromide with 0.02% ascorbic acid (Sigma, Israel), using a 10- μ L Hamilton microsyringe fitted with a 26-gauge cannula. The injection rate was 1 μ L/min and the cannula was left in place after the injection for an additional 5 min. Lesion coordinates were: anterior–posterior (AP) 4.8 mm, medial–lateral (ML) 1.6 mm, dorsal–ventral (DV) 8.4 mm from dura (Paxinos & Watson, 1986). Ten additional rats went through the same surgical procedure, but were injected with 4 μ L of saline to either the right (five rats) or the left (five rats) SNc (sham-operated rats).

After MRI measurements, 6-OHDA-lesioned rats, anesthetized with 30 mg/kg pentobarbital given *i.p.*, were perfused and tyrosine hydroxylase (TH) immunofluorescent staining (rabbit IgG 1 : 100, Chemicon, Temecula, USA) was performed on two 20- μ m frozen coronal sections of the striatum. Staining intensity was measured using Adobe Photoshop 6.0 software and the lesion side was compared with the intact side to assess lesion severity in individual animals. Only rats that were found to have a pronounced reduction (above 50%) of TH level in the striatum of the lesion side compared with the non-lesion side were further used in the analysis (five right and four left 6-OHDA-lesioned rats).

All surgical and experimental procedures were performed in accordance with the NIH Guide for the Care & Use of Laboratory Animals (1996), and with the Hebrew University guidelines for the use and care of laboratory animals in research, supervised by the institutional Animal Care and Use Committee.

MRI method and analysis

MRI measurements were performed 10–14 days after lesion induction. Rats were anaesthetized with urethane (1 g/kg *i.p.*, Sigma) and were restrained in a home-built head and body holder. Temperature was maintained with a water blanket. MRI measurements were performed with a 4.7-T Bruker Biospec system, using a 38-mm Bruker head-dedicated volume coil. For functional studies, a gradient echo planner imaging (EPI) sequence was applied to obtain coronal slices (TR = 2000 ms, TE = 22 ms, matrix size = 128 \times 128 zero filled to 256 \times 256, field of view = 4 \times 4 cm, nine slices approximately 2 to –7 mm AP, 1-mm slice thickness, resolution 156 \times 156 \times 1000 μ m³). Each data set consisted of 80 sequential images with a temporal

resolution of 2 s. Fifteen to 20 sets were acquired for each animal. Only motion-free sets were included in the analysis (approximately four per animal). Anatomical images were recorded as well, using a spin echo sequence.

Image analysis was performed using self-written software, written in IDL (Interactive Data Language, Version 5.4, Research System, Boulder, CO, USA). The first ten images of each data set were removed to ensure steady-state conditions, and a low-pass filter (0.15 Hz) was applied on the remaining images to filter cardiac and respiratory fluctuations, given that the cardiac rate is 2.6 ± 0.1 Hz and the respiratory rate is 1.33 ± 0.16 Hz, as was measured using Bruker respiratory and ECG sensors. Although this filtering does not completely remove respiratory and cardiac fluctuations, their contribution to the temporal fluctuations was negligible, given that no differences in the respiratory and cardiac rates were found between the groups. The analysis consisted of the following steps. (i) Motion exclusion: manual inspection of the data sets was performed and images with motion were removed from the sets. Note that no motion correction was used to avoid any effect on the signal fluctuations. (ii) Choosing regions of interest (ROIs): using the rat brain atlas (Paxinos & Watson, 1986), four ROIs in the coronal slices were defined for further analysis: the right and the left sensorimotor cortex, which includes the primary and the secondary motor cortex (~70 pixels), and the right/left striatum (~90 pixels). In addition, two control areas were chosen: the substantia innominata, a region which is not directly involved in the BG–cortex circuit, and a muscular region outside the brain. Both control regions were chosen in the right and the left hemispheres. Initially, additional ROIs were chosen in the globus pallidus, ventro-lateral nuclei of the thalamus and the subthalamic nucleus. However, owing to high susceptibility artefacts and low signal-to-noise ratio at these locations, no significant conclusions from these areas could be drawn. (iii) Normalization: this was performed in two steps. To correct for coil homogeneity (e.g. possible difference between the right and left hemispheres), the data were normalized with respect to the intensity of a homogeneous water sample that was measured using the same parameters as in the animal experiments. In the second step, we normalized the inter-individual variance according to the whole brain intensity (Small *et al.*, 2000). Qualitatively similar results were obtained with and without normalization, verifying that it had only a small effect on signal fluctuations. (iv) Estimation of temporal and spatial fluctuations: for each volume element, the temporal standard deviation (SD) was calculated and averaged together (hereafter the 'temporal variance'), whereas for the spatial variance, the SD of these temporal SDs in each ROI was calculated. (v) A one-tailed *t*-test between the groups was performed. Significance was set at $P < 0.05$.

Results

Figure 1 shows the group average temporal (Fig. 1A) and spatial (Fig. 1B) variance in the different ROIs of the left sham-operated and PD rat groups. Similar results were obtained for the right lesion and sham-operated groups (Table 1). A significant reduction of temporal variance was observed in both the right and the left sensorimotor cortices and striatum of the PD group as compared with the sham-operated rat group. No significant differences in the temporal variances of the control areas were found. Similarly, the average spatial variance was significantly reduced in the left and right cortices and striatum but did not exhibit significant change in the control areas.

Figure 2 presents typical temporal variance maps from a left 6-OHDA rat and from a left sham-operated rat. The temporal variance in the left 6-OHDA rat's cortex (Fig. 2c) is lower than the temporal

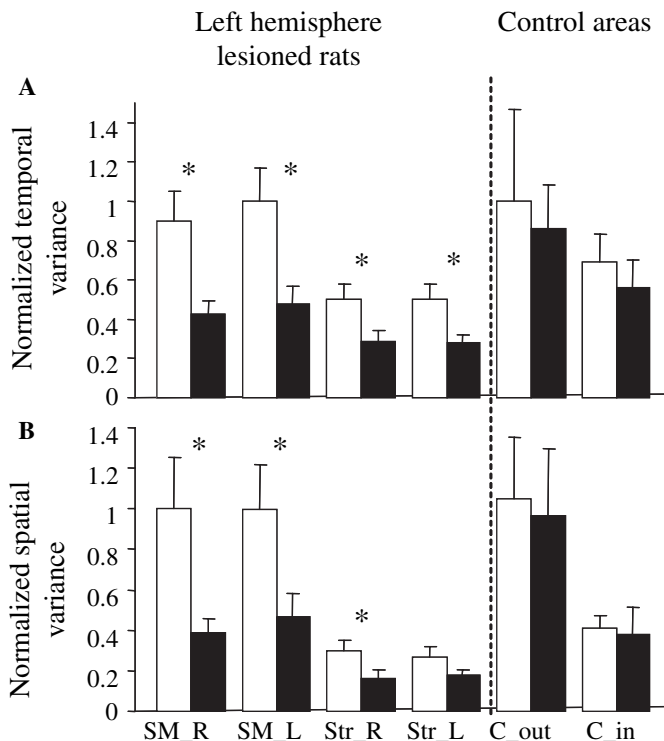


FIG. 1. Normalized temporal (A) and spatial (B) variances of 6-OHDA-treated rats (black bars) and sham-operated rats (white bars) in the left hemisphere lesioned rat groups. Error bars are mean standard errors. Values of the right (R)/left (L) sensorimotor cortex (SM), striatum (Str) and the control areas in and outside the brain (C_{in} and C_{out}, respectively) are shown. Data are normalized according to SM_R. * $P < 0.05$.

TABLE 1. P -values for the comparisons between sham-operated and 6-OHDA rat groups for the different ROIs

| | Right 6-OHDA-lesioned vs. sham-operated | | Left 6-OHDA-lesioned vs. sham-operated | |
|---------------------------|---|----------------------|--|----------------------|
| | Temporal fluctuations | Spatial fluctuations | Temporal fluctuations | Spatial fluctuations |
| Right sensorimotor cortex | 0.0145 | 0.0637 | 0.0059 | 0.0151 |
| Left sensorimotor cortex | 0.0647 | 0.156 | 0.00645 | 0.0222 |
| Right striatum | 0.0720 | 0.0329 | 0.0187 | 0.0268 |
| Left striatum | 0.0946 | 0.115 | 0.0123 | 0.0645 |
| Control in | 0.267 | 0.409 | 0.395 | 0.426 |
| Control out | 0.140 | 0.332 | 0.0964 | 0.257 |

Control in, substantia innominata; Control out, muscles outside the brain.

variance in the left sham-operated rat's cortex (Fig. 2b), whereas the smaller difference in the striatum is not seen in these maps.

All statistical analyses, for all groups and all the ROIs, are presented in Table 1, which shows that both temporal and spatial variances have undergone a bilateral reduction following a unilateral lesion.

To test whether the reduction in basal temporal and spatial variances was more pronounced in the lesion hemisphere, we subtracted the average temporal and spatial variances in the 6-OHDA rat group from the average variances in the sham-operated rat group for all ROIs in the left and in the right lesion groups (Fig. 3). The observed

differences for the temporal variance suggest that basal activity level was more reduced in the lesion hemisphere although it failed to reach significance. No such differences were found for the spatial variance.

Discussion

Our hypothesis in estimating basal neuronal activity and synchronization levels is that the temporal fluctuation of a single voxel in MRI BOLD contrast is proportional to its average neuronal activity. It is based on the assumption that a voxel's temporal fluctuation in high spatial resolution MRI data (where large blood vessels can be excluded) originates from capillary blood flow that is neuronally regulated. We further assume that vascular fluctuations that are not neuronally regulated are either negligible (Goelman, 2004; Pelled & Goelman, 2004) or have a comparable effect on control and PD rats, and thus have minimal impact on the group comparison. Taken together, these features mean that (1) the temporal variance of an MRI voxel estimates its average activity and (2) the variance of these activities in a predefined region (the 'spatial variance') reflects the homogeneity of the region defined here as 'functional homogeneity'. Based on these assumptions the correlation between temporal variances and basal activity level seems straightforward; however, the physiological meaning of 'spatial variance' or 'functional homogeneity' is more complex. Intuitively, one can imagine a region for which the volume elements have uncorrelated neuronal activity. The spatial variance of this region will be higher than the spatial variance of a region for which the activity of its volume elements is highly correlated. In other words, a region of inhomogeneous activity will result in higher spatial variance than a region of homogeneous activity. A region of highly synchronized neuronal activity will cause correlated capillary blood flow fluctuations and will subsequently have low spatial variance or high 'functional homogeneity' compared with a region of low synchronized activity. Therefore, although 'functional homogeneity' of a region is not equivalent to the average neuronal synchronization in that region, because the latter is defined by temporal correlations between sites, we suggest that it relates to the average neuronal synchronization and can be used to estimate synchronization changes between groups. We are aware, however, that our basic assumption of the link between neuronal activity and BOLD signal fluctuations could be significantly strengthened by other modalities such as optical imaging, electrophysiology or blood flow measurements, each with its own limitations, and future effort will be given to accumulate such data.

Other studies have measured basal neuronal activity levels and their relationship to the BOLD fMRI signal by calculating the oxygen cerebral metabolic rate together with electrophysiological recording while manipulating the level of anaesthesia (Hyder *et al.*, 2002; Smith *et al.*, 2002). In addition, the basal neuronal activity level has been estimated by measuring the glutamate–glutamine flux with ^{13}C nuclear magnetic resonance imaging (Shulman *et al.*, 2001a,b). In line with our assumptions, these studies hypothesized that ΔBOLD (the BOLD fMRI signal difference between stimulation ON and stimulation OFF) depends on the basal neuronal activity level, as stimulation induces a particular magnitude of activity. Recent findings of no significant differences in the BOLD response for different halothane anaesthesia levels but substantial variation in the extent and magnitude of the BOLD response over time for α -chloralose anaesthesia (Austin *et al.*, 2005) suggest that this effect might be dependent upon anaesthesia type and level.

It could be argued that our observation of reduced basal activity level in PD rats is the outcome of the reduction in dopamine levels, as dopamine plays an important role in cortical microcirculation (Krimer *et al.*, 1998). However, although cortical reduction in dopamine level

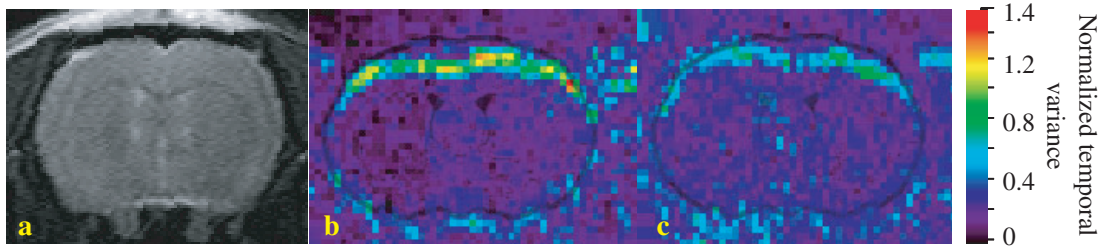


FIG. 2. BOLD temporal variance maps of left sham-operated (b) and left 6-OHDA (c) representative rats. A reference image showing the sensorimotor cortex and the striatum is shown on the left (a). Reduced temporal variance in the sensorimotor cortex is observed in the 6-OHDA rat compared with the sham-operated rat. The intensity scale is comparable with Fig. 1.

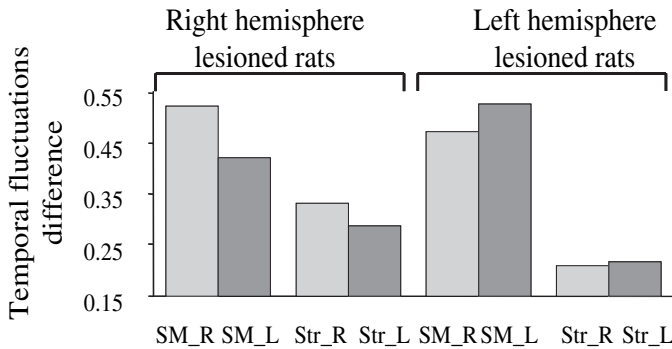


FIG. 3. Difference in the average temporal variance for ROI in the right (R)/left (L) sensorimotor cortex (SM) and in the striatum (Str). These differences were calculated by subtracting the average temporal variance of the PD group from the sham-operated group, for each ROI. Light grey bars represent right areas and dark grey bars left areas.

was found in PD patients (Scatton *et al.*, 1982) and in MPTP-treated (1-methyl-4-phenyl-1,2,3,6-tetrahydropyridine) monkeys (Elsworth *et al.*, 1990), no changes in D1 and D2 dopamine receptors have been found in the unilateral 6-OHDA rat model (Yokoyama & Okamura, 1997; Araki *et al.*, 1998). Therefore, our findings reflect a real change in neuronal activity and not a global change in microcirculation.

The reduction in basal activity levels found here in the Parkinsonian state (Fig. 1A) is in line with classical models, and with studies using autoradiography measurements of the regional cerebral metabolic rate

of glucose (rCMRglucose) that report decreased rCMRglucose in the sensory and motor regions in the lesioned hemisphere of the unilateral PD rat model (Carlson *et al.*, 1999), and the bilateral MPTP primate PD model (Palombo *et al.*, 1988, 1990). Furthermore, bilaterally decreased rCMRglucose has been found in the striatum of the unilateral PD rat model (Schwartz & Huston, 1996) and in the unilateral monkey PD model (Palombo *et al.*, 1988, 1990). Our other finding, the increased spatial homogeneity that we suggest results from increased neuronal synchronization, is also in line with other physiological studies. For example, high neuronal synchronization in the motor cortex in the MPTP PD primate model has been observed (Goldberg *et al.*, 2002), as well as increased neuronal synchronization in the globus pallidus and in the subthalamic nucleus in human PD patients and in MPTP monkeys (Hurtado *et al.*, 1999; Levy *et al.*, 2000; Heimer *et al.*, 2002).

The contrasting results between some of the functional neuro-imaging studies and classical BG–cortex circuit models can therefore be explained by assuming that stimulation causes peak capillary flow of approximately the same level in PD and healthy states. Thus the reduction in basal neuronal activity level can account for the over-activation observed in functional neuro-imaging studies. This point is illustrated in Fig. 4. In the PD brain, the sensorimotor cortex neurons receive less excitatory input from the thalamus and therefore their spontaneous firing rate is reduced. Assuming a similar capillary flow level during stimulation for both normal and PD conditions, sensory or sensory/motor stimulation will produce an increased functional neuro-imaging signal compared with the normal brain.

Another important finding is the bilateral response observed in the PD state. This bi-hemispheric abnormal behaviour was observed in

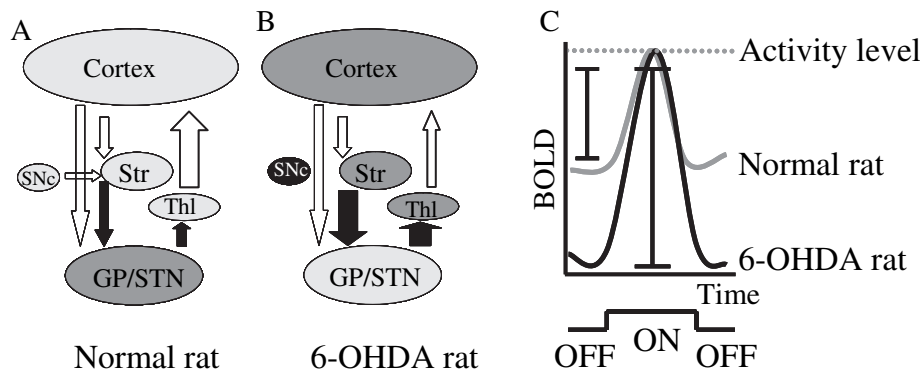


FIG. 4. Illustration of the basal ganglia–cortex circuitry in healthy and PD rats and its effect on the BOLD signal. (A) The interactions in the normal brain. (B) The interactions in the PD brain: SNc lesion and striatal dopamine depletion result in a decrease in excitatory input to the cortex. (C) Activity diagram: for a fixed activity during stimulation, Δ BOLD is higher in the 6-OHDA rat group (black trace) owing to the lower base level of 6-OHDA. Str, striatum; GP, globus pallidus; STN, subthalamic nucleus; Tha, thalamus; SNc, substantia nigra pars compacta; ON, stimulation segment; OFF, rest segment.

our previous study using the unilateral rat model (Pelled *et al.*, 2002), in studies using rCMRglucose methods (Palombo *et al.*, 1990) and in hemi-Parkinsonian patients (Thobois *et al.*, 2000). This phenomenon can be explained by functional amplification of projections from the BG output nuclei (globus pallidus internal segment/substantia nigra pars reticulata) to the contralateral thalamic area (Parent & Hazrati, 1995; Gerfen & Wilson, 1996) in PD. As expected, however, the reduction in basal activity (but not in synchronization level) tends to be more pronounced in the lesioned hemisphere (Fig. 2).

In conclusion, we applied a simple non-invasive MRI method to estimate the difference in the average neuronal activation and synchronization levels between groups. We used this method to compare the basal activity level in PD model rats versus control rats. This comparison shows a bilateral reduction in the basal activity level in PD, in line with the classical models of BG circuitry (Albin *et al.*, 1989; DeLong, 1990; Mink & Thach, 1991). Moreover, our results help to provide an explanation for the variations between this model and some functional imaging studies. In addition, we obtained an increase in functional homogeneity in the PD state that is interpreted as an increase in functional synchronization. We are aware that our interpretation is based on the hypothesis linking the temporal BOLD signal fluctuations to neuronal activity. However, by comparing two groups known to differ in their neuronal activity, which presumably do not differ in their vascular modulation, we can safely argue that our findings reflect differences in neuronal activity. The fact that our results provide additional support for the Albin-DeLong model and can resolve some of the contradictions with functional neuro-imaging lends weight to this interpretation. The simplicity and non-invasiveness of this methodology make it a good candidate as an objective tool to measure the severity of disease and enable follow-ups and evaluations of treatment effectiveness in human PD patients.

Acknowledgements

This study was supported by the Israel Science Foundation (grant no. 596/01) and partly by the Dana Foundation, the Israel Ministry of Sciences and the BMBF Israel-Germany collaboration in medical research.

Abbreviations

6-OHDA, 6-hydroxydopamine; BG, basal ganglia; BOLD, blood oxygenation level dependent; EPI, echo planner imaging; fMRI, functional magnetic resonance imaging; MPTP, 1-methyl-4-phenyl-1,2,3,6-tetrahydropyridine; PD, Parkinson's disease; PET, positron emission tomography; rCMRglucose, regional cerebral metabolic rate of glucose; ROI, region of interest; SNc, substantia nigra pars compacta; SPECT, single photon emission tomography; TE, echo time; TH, tyrosine hydroxylase; TR, repetition time.

References

- Albin, R.L., Young, A.B. & Penney, J.B. (1989) The functional anatomy of basal ganglia disorders. *Trends Neurosci.*, **12**, 366–375.
- Araki, T., Tanji, H., Kato, H. & Itoyama, Y. (1998) Sequential changes of dopaminergic receptors in the rat brain after 6-hydroxydopamine lesions of the medial forebrain bundle. *J. Neurol. Sci.*, **160**, 121–127.
- Austin, V.C., Blamire, A.M., Allers, K.A., Sharp, T., Styles, P., Matthews, P.M. & Sibson, N.R. (2005) Confounding effects of anesthesia on functional activation in rodent brain: a study of halothane and alpha-chloralose anesthesia. *Neuroimage*, **24**, 92–100.
- Biswal, B., Van Kylen, J. & Hyde, J.S. (1997) Simultaneous assessment of flow and BOLD signals in resting-state functional connectivity maps. *NMR Biomed.*, **10**, 165–170.

- Biswal, B., Yetkin, F.Z., Haughton, V.M. & Hyde, J.S. (1995) Functional connectivity in the motor cortex of resting human brain using echo-planar MRI. *Magn. Reson. Med.*, **34**, 537–541.
- Brooks, D.J. (1999) Functional imaging of Parkinson's disease: is it possible to detect brain areas for specific symptoms? *J. Neural Transm. Suppl.*, **56**, 139–153.
- Buchel, C. & Friston, K.J. (1997) Modulation of connectivity in visual pathways by attention: cortical interactions evaluated with structural equation modelling and fMRI. *Cereb. Cortex*, **7**, 768–778.
- Buchel, C. & Friston, K.J. (1998) Dynamic changes in effective connectivity characterized by variable parameter regression and Kalman filtering. *Hum. Brain Mapp.*, **6**, 403–408.
- Carlson, J.D., Pearlstein, R.D., Buchholz, J., Iacono, R.P. & Maeda, G. (1999) Regional metabolic changes in the pedunculo-pontine nucleus of unilateral 6-hydroxydopamine Parkinson's model rats. *Brain Res.*, **828**, 12–19.
- Catalan, M.J., Ishii, K., Honda, M., Samii, A. & Hallett, M. (1999) A PET study of sequential finger movements of varying length in patients with Parkinson's disease. *Brain*, **122**, 483–495.
- DeLong, M.R. (1990) Primate model of movement disorders of the basal ganglia origin. *Trends Neurosci.*, **13**, 281–285.
- Elsworth, J.D., Deutch, A.Y., Redmond, D.E. Jr, Sladek, J.R. Jr & Roth, R.H. (1990) MPTP reduces dopamine and norepinephrine concentrations in the supplementary motor area and cingulate cortex of the primate. *Neurosci. Lett.*, **114**, 316–322.
- Gerfen, C.R. & Wilson, C.J. (1996) The basal ganglia. In Swanson, L.W., Bjurklund, A. & Hokfelt, T. (Eds), *Handbook of Chemical Neuroanatomy*. Elsevier Science, New York, pp. 371–468.
- Goelman, G. (2004) Radial correlation contrast – a functional connectivity MRI contrast to map changes in local neuronal communication. *Neuroimage*, **23**, 1432–1439.
- Goldberg, J.A., Boraud, T., Maraton, S., Haber, S.N., Vaadia, E. & Bergman, H. (2002) Enhanced synchrony among primary motor cortex neurons in the 1-methyl-4-phenyl-1,2,3,6-tetrahydropyridine primate model of Parkinson's disease. *J. Neurosci.*, **22**, 4639–4653.
- Heimer, G., Bar-Gad, I., Goldberg, J.A. & Bergman, H. (2002) Dopamine replacement therapy reverses abnormal synchronization of pallidal neurons in the 1-methyl-4-phenyl-1,2,3,6-tetrahydropyridine primate model of parkinsonism. *J. Neurosci.*, **22**, 7850–7855.
- Hurtado, J.M., Gray, C.M., Tamas, L.B. & Sigvardt, K.A. (1999) Dynamics of tremor-related oscillations in the human globus pallidus: a single case study. *Proc. Natl Acad. Sci. USA*, **96**, 1674–1679.
- Hyder, F., Rothman, D.L. & Shulman, R.G. (2002) Total neuroenergetics support localized brain activity: implications for the interpretation of fMRI. *Proc. Natl Acad. Sci. USA*, **99**, 10771–10776.
- Jahanshahi, M., Jenkins, I.H., Brown, R.G., Marsden, C.D., Passingham, R.E. & Brooks, D.J. (1995) Self-initiated versus externally triggered movements. I. An investigation using measurement of regional cerebral blood flow with PET and movement-related potentials in normal and Parkinson's disease subjects. *Brain Res.*, **118**, 913–933.
- Jenkins, I.H., Fernandez, W., Playford, E.D., Lees, A.J., Frackowiak, R.S., Passingham, R.E. & Brooks, D.J. (1992) Impaired activation of the supplementary motor area in Parkinson's disease is reversed when akinesia is treated with apomorphine. *Ann. Neurol.*, **32**, 749–757.
- Krimer, L.S., Muly, E., 3rd, Williams, G.V. & Goldman-Rakic, P.S. (1998) Dopaminergic regulation of cerebral cortical microcirculation. *Nat. Neurosci.*, **1**, 286–289.
- Kruger, G. & Glover, G.H. (2001) Physiological noise in oxygenation-sensitive magnetic resonance imaging. *Magn. Reson. Med.*, **46**, 631–637.
- Levy, R., Hutchison, W.D., Lozano, A.M. & Dostrovsky, J.O. (2000) High-frequency synchronization of neuronal activity in the subthalamic nucleus of parkinsonian patients with limb tremor. *J. Neurosci.*, **20**, 7766–7775.
- Mink, J.W. & Thach, W.T. (1991) Basal ganglia motor control. I. Nonexclusive relation of pallidal discharge to five movement modes. *J. Neurophysiol.*, **65**, 273–300.
- Palombo, E., Porrino, L.J., Bankiewicz, K.S., Crane, A.M., Kopin, I.J. & Sokoloff, L. (1988) Administration of MPTP acutely increases glucose utilization in the substantia nigra of primates. *Brain Res.*, **453**, 227–234.
- Palombo, E., Porrino, L.J., Bankiewicz, K.S., Crane, A.M., Sokoloff, L. & Kopin, I.J. (1990) Local cerebral glucose utilization in monkeys with hemiparkinsonism induced by intracarotid infusion of the neurotoxin MPTP. *J. Neurosci.*, **10**, 860–869.
- Parent, A. & Hazrati, L.N. (1995) Functional anatomy of the basal ganglia. I. The cortico-basal ganglia-thalamo-cortical loop. *Brain Res. Rev.*, **20**, 91–127.
- Paxinos, G. & Watson, C. (1986) *The Rat Brain in Stereotaxic Coordinates*. Academic Press, New York.

- Pelled, G., Bergman, H. & Goelman, G. (2002) Bilateral overactivation of the sensorimotor cortex in the unilateral rodent model of Parkinson's disease – a functional magnetic resonance imaging study. *Eur. J. Neurosci.*, **15**, 389–394.
- Pelled, G. & Goelman, G. (2004) Different physiological MRI noise between cortical layers. *Magn. Reson. Med.*, **52**, 913–916.
- Playford, E.D., Jenkins, I.H., Passingham, R.E., Nutt, J., Frackowiak, R.S. & Brooks, D.J. (1992) Impaired mesial frontal and putamen activation in Parkinson's disease: a positron emission tomography study. *Ann. Neurol.*, **32**, 151–161.
- Rascol, O., Sabatini, U., Fabre, N., Brefel, C., Loubinoux, I., Clesis, P., Senard, J.M., Montastruc, J.L. & Chollet, F. (1997) The ipsilateral cerebellar hemisphere is overactive during hand movements in akinetic parkinsonian patients. *Brain*, **120**, 103–110.
- Sabatini, U., Boulanouar, K., Fabre, N., Martin, F., Carel, C., Colonnese, C., Bozzao, L., Berry, I., Montastruc, J.L., Chollet, F. & Rascole, O. (2000) Cortical motor reorganization in akinetic patients with Parkinson's disease: a functional MRI study. *Brain*, **123**, 394–403.
- Scatton, B., Rouquier, L., Javoy-Agid, F. & Agid, Y. (1982) Dopamine deficiency in the cerebral cortex in Parkinson disease. *Neurology*, **32**, 1039–1040.
- Schwartz, R.K. & Huston, J.P. (1996) Unilateral 6-hydroxydopamine lesions of meso-striatal dopamine neurons and their physiological sequelae. *Prog. Neurobiol.*, **49**, 215–266.
- Shulman, R.G., Hyder, F. & Rothman, D.L. (2001a) Cerebral energetics and the glycogen shunt: neurochemical basis of functional imaging. *Proc. Natl Acad. Sci. USA*, **98**, 6417–6422.
- Shulman, R.G., Hyder, F. & Rothman, D.L. (2001b) Lactate efflux and the neuroenergetic basis of brain function. *NMR Biomed.*, **14**, 389–396.
- Small, S.A., Wu, E.X., Bratsch, D., Perera, G.M., Lacefield, C.O., DeLaPaz, R., Mayeux, R., Stern, Y. & Kandel, E.R. (2000) Imaging physiologic dysfunction of individual hippocampal subregions in human and genetically modified mice. *Neuron*, **28**, 653–664.
- Smith, A.J., Blumenfeld, H., Behar, K.L., Rothman, D.L., Shulman, R.G. & Hyder, F. (2002) Cerebral energetics and spiking frequency: the neurophysiological basis of fMRI. *Proc. Natl Acad. Sci. USA*, **99**, 10765–10770.
- Thobois, S., Dominey, P., Decety, J., Pollak, P., Gregoire, M.C. & Broussolle, E. (2000) Overactivation of primary motor cortex is asymmetrical in hemiparkinsonian patients. *Neuroreport*, **11**, 785–789.
- Yokoyama, C. & Okamura, H. (1997) Self-injurious behavior and dopaminergic neuron system in neonatal 6-hydroxydopamine-lesioned rat: 1. Dopaminergic neurons and receptors. *J. Pharmacol. Exp. Ther.*, **280**, 1016–1030.